ISSN 1674-1056
http://cpb.iphy.ac.cn
http://iopscience.iop.org/cpb
中国物理 B
Chinese Physics
中国物理 Chinese Physics B

Optimization of a magneto-optic trap using nanofibers

Xin Wang(王鑫)[1], Li-Jun Song(宋丽军)[1], Chen-Xi Wang(王晨曦)[1], Peng-Fei Zhang(张鹏飞)[1,2], Gang Li(李刚)[1,2], Tian-Cai Zhang(张天才)[1,2]

Citation: Chin. Phys. B . 2019, 28(7): 073701. **doi:** 10.1088/1674-1056/28/7/073701
Journal homepage: http://cpb.iphy.ac.cn; http://iopscience.iop.org/cpb

What follows is a list of articles you may be interested in

Optimization of endcap trap for single-ion manipulation

Yuan Qian(钱源), Chang-Da-Ren Fang(方长达人), Yao Huang(黄垚), Hua Guan(管桦), Ke-Lin Gao(高克林)
Chin. Phys. B . 2018, 27(6): 063701. **doi:** 10.1088/1674-1056/27/6/063701

Investigation and optimization of sampling characteristics of light field camera for flame temperature measurement

Yudong Liu(刘煜东), Md. Moinul Hossain, Jun Sun(孙俊), Biao Zhang(张彪), Chuanlong Xu(许传龙)
Chin. Phys. B . 2019, 28(3): 034207. **doi:** 10.1088/1674-1056/28/3/034207

Resonantly driven exciton Rabi oscillation in single quantum dots emitting at 1300 nm

Yong-Zhou Xue(薛永洲), Ze-Sheng Chen(陈泽升), Hai-Qiao Ni(倪海桥), Zhi-Chuan Niu(牛智川), De-Sheng Jiang(江德生), Xiu-Ming Dou(窦秀明), Bao-Quan Sun(孙宝权)
Chin. Phys. B . 2017, 26(8): 084202. **doi:** 10.1088/1674-1056/26/8/084202

Optical manipulation of gold nanoparticles using an optical nanofiber

Li Ying, Hu Yan-Jun
Chin. Phys. B . 2013, 22(3): 034206. **doi:** 10.1088/1674-1056/22/3/034206

Optimum design of photoresist thickness for 90-nm critical dimension based on ArF laser lithography

Chen De-Liang, Cao Yi-Ping, Huang Zhen-Fen, Lu Xi, Zhai Ai-Ping
Chin. Phys. B . 2012, 21(8): 084201. **doi:** 10.1088/1674-1056/21/8/084201

Optimization of a magneto–optic trap using nanofibers*

Xin Wang(王鑫)[1], Li-Jun Song(宋丽军)[1], Chen-Xi Wang(王晨曦)[1], Peng-Fei Zhang(张鹏飞)[1,2,†], Gang Li(李刚)[1,2], and Tian-Cai Zhang(张天才)[1,2,‡]

[1] *State Key Laboratory of Quantum Optics and Quantum Optics Devices, Institute of Opto-Electronics, Shanxi University, Taiyuan* 030006, *China*
[2] *Collaborative Innovation Center of Extreme Optics, Shanxi University, Taiyuan* 030006, *China*

(Received 28 February 2019; revised manuscript received 7 May 2019; published online 25 June 2019)

We experimentally demonstrate a reliable method based on a nanofiber to optimize the number of cold atoms in a magneto–optical trap (MOT) and to monitor the MOT in real time. The atomic fluorescence is collected by a nanofiber with subwavelength diameter of about 400 nm. The MOT parameters are experimentally adjusted in order to match the maximum number of cold atoms provided by the fluorescence collected by the nanofiber. The maximum number of cold atoms is obtained when the intensities of the cooling and re-pumping beams are about 23.5 mW/cm^2 and 7.1 mW/cm^2, respectively; the detuning of the cooling beam is -13.0 MHz, and the axial magnetic gradient is about 9.7 Gauss/cm. We observe a maximum photon counting rate of nearly $(4.5 \pm 0.1) \times 10^5$ counts/s. The nanofiber–atom system can provide a powerful and flexible tool for sensitive atom detection and for monitoring atom–matter coupling. It can be widely used from quantum optics to quantum precision measurement.

Keywords: nanofiber, magneto–optic trap, optimization, fluorescence, efficient coupling

PACS: 37.10.–x, 42.81.Qb, 32.50.+d, 42.50.–p **DOI:** 10.1088/1674-1056/28/7/073701

1. Introduction

Nanofibers with an ultrathin waist at subwavelength level can offer a strong transverse confinement of the guided modes, which leads to the spread of a powerful evanescent field surrounding the waist.[1] During the past decade, nanofibers have been a topic of great interest and have been widely applied in many fields, such as quantum photonics, optical sensing, precision measurement, and quantum optics.[2–5] Nanofibers can be fabricated by stretching a standard single-mode fiber while heating it with a hydrogen/oxygen flame. Both ends of the single-mode fiber are fixed on two motors. The process of stretching the single-mode fiber is precisely controlled by a computer so the normal fibers are tapered adiabatically.[6] Only fundamental modes can propagate in the nanofibers because they have subwavelength diameters. The evanescent field outside the nanofiber reaches its maximum around $ka = 1.45$,[7] where k is the wave number in free space and a is the nanofiber radius.

The magneto–optic trap (MOT) is a powerful tool to effectively manipulate the cold atoms, and cold atoms have been widely applied in quantum physics experiments[8–10] such as those involving Rydberg atoms,[11,12] ultra-cold atoms,[13,14] cavity quantum electrodynamics,[15,16] and hybrid quantum systems.[17] In the experiments mentioned above, it is desirable to start with a MOT containing as many atoms as possible. The number of atoms depends on the MOT parameters, including the intensities of MOT beams, the detuning of cooling beams, and the magnetic field gradient. Two traditional techniques are applied to measure the number of cold atoms in a MOT:[18] (i) absorption imaging and (ii) fluorescence imaging. The two methods can be used to optimize the MOT parameters.[19–23] Typically, an optical lens is used to collect the atomic fluorescence or collect photons absorbed by the cold atom cloud. There are two disadvantages for these two traditional techniques. One is that the atoms in the MOT are destroyed when the absorption imaging technique is used to optimize the MOT. Thus the MOT cannot be optimized in real time. Another is that the collection efficiency is usually low for the fluorescence imaging technique. Thus, these techniques cannot be used effectively for mini-MOTs that have a small number of atoms. Since a nanofiber can significantly enhance the coupling efficiency of atomic fluorescence when the atoms are within the evanescent field of the nanofibers,[7,24,25] it is a powerful tool for collecting the fluorescence from cold atoms in a MOT.[26] Theoretically, the coupling efficiency for a single atom on a nanofiber surface can reach more than 20%,[7] which has been demonstrated experimentally.[27,28] Nanofibers can thus be used to optimize a MOT according to the atomic fluorescence collected by the nanofiber when it is overlapped with the MOT, even though the number of atoms in a MOT is very small. Targeted toward increasing the coupling efficiency, methods for various nanofiber-based cavities have been demonstrated in recent years.[29–34]

In this paper, we experimentally demonstrate a nanofiber-

*Project supported by the National Key Research and Development Program of China (Grant No. 2017YFA0304502), the National Natural Science Foundation of China (Grant Nos. 11574187, 11634008, 11674203, and 61227902), and the Fund for Shanxi "1331 Project", China.

†Corresponding author. E-mail: cqedpfzhang@163.com
‡Corresponding author. E-mail: tczhang@sxu.edu.cn

based method of optimizing a MOT. Atomic fluorescence is collected very efficiently by a nanofiber with a subwavelength diameter. We optimize the MOT parameters according to the fluorescence collected by the nanofiber including the intensity of MOT beams, the detuning of cooling beams, and the magnetic field gradient. We can obtain the optimal parameters for the maximum number of cold atoms in the MOT. In addition, we can monitor the number of cold atoms in the MOT in real time.

2. Experimental setup

Figure 1 is a schematic of the coupling between a nanofiber and a MOT. We fabricate the nanofiber with waist diameters around 400 nm using the flame-brush method[31,35,36] from a single-mode fiber (SM800, Fibercore, Southampton, UK). The nanofiber transmission can reach more than 95%. We put the nanofiber into an ultra-high vacuum chamber via an optical fiber feedthrough.[37] A conventional MOT is positioned in the center of the chamber.[38] The cooling beam is from an extended cavity diode laser (DL-100, Toptica, Munich, Germany), which is tuned several megahertz below the transition of $6^2S_{1/2}$, $F = 4 \rightarrow 6^2P_{3/2}$, $F' = 5$ for cesium. The re-pumping beam is from a self-made diode laser, which resonates to the transition of $6^2S_{1/2}$, $F = 3 \rightarrow 6^2P_{3/2}$, $F' = 4$ for cesium. The cooling beam is coupled to an optical fiber that maintains its polarization. It is then split into three beams. The re-pumping beam is combined with one of the cooling beams. The diameter of each beam is 6.1 ± 0.1 mm. The beams are circularly polarized with the retro-reflected beams possessing the opposite circular polarization. The quadrupole magnetic field provided by anti-Helmholtz coils can be adjusted by changing the current in the coils. The nanofiber is kept in place with a silica holder, which is fixed to a piezo stage. We can move the nanofiber to exactly overlap with the MOT using the piezo stage. The atomic fluorescence collected by the nanofiber is detected with a single photon counting module (SPCM, SPCM-800-14-FC, Excelitas, Massachusetts, USA) connected to one end of the fiber.

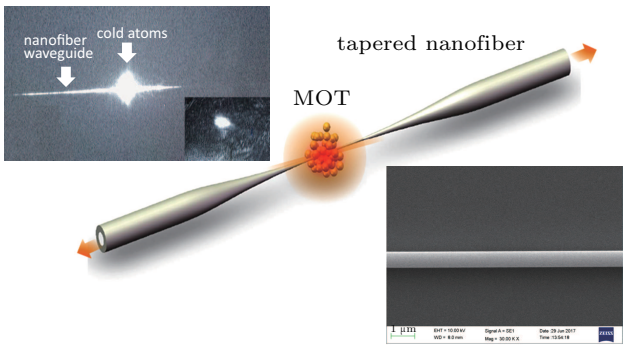

Fig. 1. Schematic diagram of the experimental setup: the nanofiber overlaps with the cold atom cloud. The upper-left figure shows the CCD image of cold atoms and the nanofiber. The lower-right figure shows a typical SEM image of a nanofiber.

The upper-left figure in Fig. 1 shows the image of cold atoms and nanofiber taken by a charge-coupled device (CCD). The lower-right figure in Fig. 1 shows a typical scanning electron microscope (SEM) image of a nanofiber.

3. Experimental results

3.1. Atomic fluorescence measurement

We plot the photon counting rate from the SPCM versus time as shown in Fig. 2. Three steps with different counting rate levels correspond to three experimental setups. The first step of five seconds corresponds to the experiment wherein all of the MOT beams and the magnetic field are switched off (condition 1 shown in Fig. 2). The counts are due to the light scattering from the background and the dark counts of the SPCM. The average counting rate for condition 1 is $(5.0 \pm 1.0) \times 10^2$ counts/s. For the second step of five seconds, all of the MOT beams are switched on and the magnetic field is still switched off (condition 2 shown in Fig. 2). In this case, no atoms are trapped yet in the MOT. We can observe only the scattering photons from MOT beams that are channeled into the nanofiber. The average counting rate in this case is $(4.9 \pm 0.5) \times 10^5$ counts/s. For the last step, both the MOT beams and the magnetic field are switched on (condition 3 shown in Fig. 2). We can observe a considerable net increase in the counting rate, which is $(4.5 \pm 0.1) \times 10^5$ counts/s. The net increase of the fluorescence is from the emission of the cold atoms trapped in the MOT excited by MOT beams. In this case, the intensity of cooling beams is 33.6 mW/cm^2, while the intensity of the re-pumping beam is 35.4 mW/cm^2. The detuning of the cooling beam is -13.0 MHz, and the axial magnetic gradient is 11.7 Gauss/cm. The current of the atomic dispenser (AS-Cs-100-F, Alvatech, Althofen, Austria) is 4.75 A.

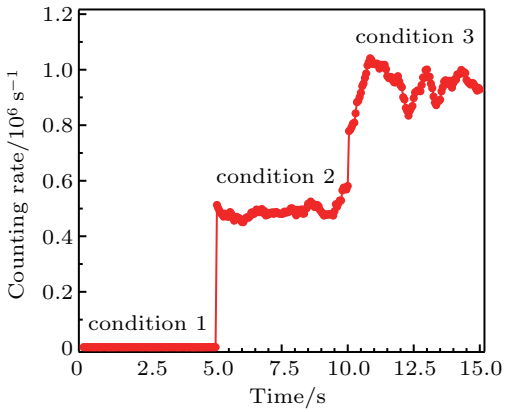

Fig. 2. Counting rate of the SPCM from atomic fluorescence collected by the nanofiber versus time for three experimental conditions. In condition 1, all the MOT beams and magnetic field are switched off. In condition 2, all the MOT beams are switched on and the magnetic field is still switched off. In condition 3, all the MOT beams and the magnetic field are switched on.

3.2. Optimization of the MOT

The increase in the counting rate shown in Fig. 2 depends on the number of cold atoms in the MOT. Thus, we can optimize the number of cold atoms by adjusting the MOT parameters, including intensities of MOT beams, magnetic field gradient, and detuning of the cooling beams. In Fig. 3(a), we plot the photon counting rate collected by the nanofiber as a function of the intensity of the cooling beams when the intensity of the re-pumping beam is 35.4 mW/cm^2. Figure 3(b) shows the counting rate as a function of the intensity of the re-pumping beams when the intensity of the cooling beam is 33.6 mW/cm^2. For both Figs. 3(a) and 3(b), the detuning of the cooling beam is -11.6 MHz and the axial magnetic gradient is 11.7 Gauss/cm. The current of the atomic dispenser is 4.75 A. The error bars are derived from the standard deviation of ten measurements, which are the same as other measurement results below. In Fig. 3, we can see that the counting rate increases in the beginning as the intensities of the cooling beams and re-pumping beam increase. The number of atoms is saturated when the intensities of the cooling beams and re-pumping beam are more than about 23.5 mW/cm^2 and 7.1 mW/cm^2, respectively.

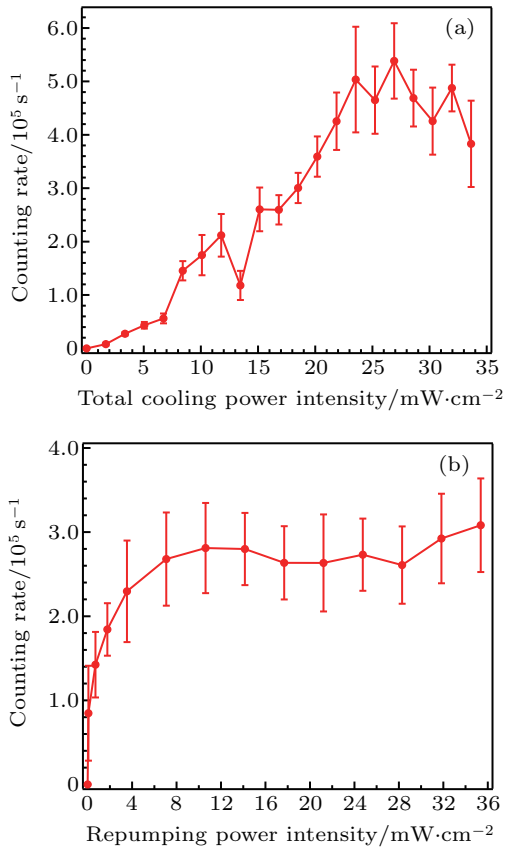

Fig. 3. (a) Counting rate from the fluorescence of cold atoms as a function of the intensity of the cooling beams. The intensity of the re-pumping beam is 35.4 mW/cm^2. (b) Counting rate from the fluorescence of cold atoms as a function of the intensity of the re-pumping beams. The intensity of the cooling beam is 33.6 mW/cm^2. The detuning of the cooling beam is -11.6 MHz and the axial magnetic gradient is 11.7 Gauss/cm for both cases.

The number of atoms remains constant until the intensities reach 33.6 mW/cm^2 and 35.4 mW/cm^2, which are the maximum intensities the lasers can provide. This is due to the saturated power for transition probabilities between different sub-levels of $6^2S_{1/2}$, $F = 4 \rightarrow 6^2P_{3/2}$, $F' = 5$. Thus, the scattered forces from the cooling beams reach saturation and the number of cold atoms approaches a constant.[39,40]

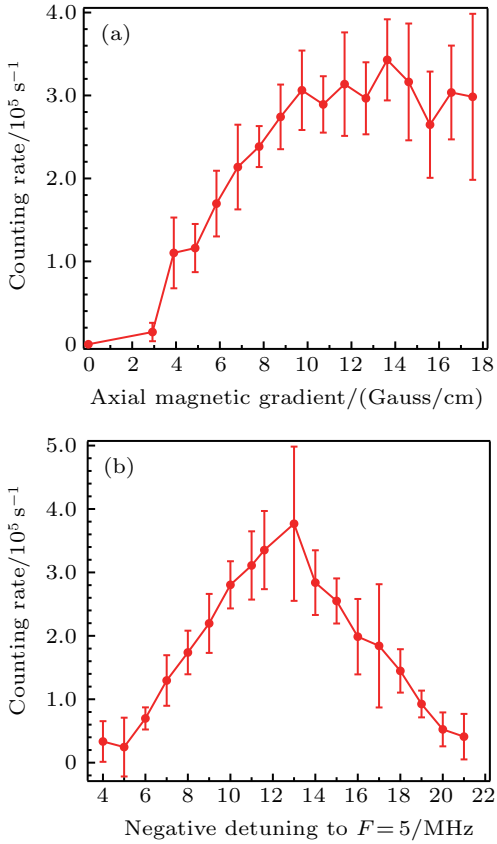

Fig. 4. (a) Counting rate from the fluorescence of cold atoms as a function of axial magnetic gradient. The detuning of cooling beams is -11.6 MHz. (b) Counting rate from the fluorescence of cold atoms as a function of detuning. The axial magnetic gradient is 11.7 Gauss/cm. The intensities of cooling and re-pumping beams are 33.6 mW/cm^2 and 35.4 mW/cm^2 for both figures.

Because the number of atoms is saturated when the intensities of the cooling beams and re-pumping beam are higher than 23.5 mW/cm^2 and 7.1 mW/cm^2, respectively, the intensities of the cooling beams and the re-pumping beam are set to 33.6 mW/cm^2 and 35.4 mW/cm^2, respectively. This can eliminate the effect of laser power fluctuation on the number of atoms in the MOT. After setting appropriate saturated intensity of MOT beams, the number of atoms is optimized by adjusting the magnetic field gradient. The measurement results are shown in Fig. 4(a). Owing to the contraction of the MOT size and the increase in density of cold atoms in the MOT with higher magnetic field gradient, the number of cold atoms in the MOT approaches a constant.[41] The counting rate is saturated when the magnetic field gradient reaches around 9.7 Gauss/cm. We fix the magnetic field gradient at 11.7 Gauss/cm, and then scan the frequency of the cooling

beams to optimize the detuning. Figure 4(b) shows the counting rate as a function of the detuning of cooling beams. We can see that the fluorescence reaches a maximum at −13.0 MHz when the transition is $6^2S_{1/2}$, $F = 4 \rightarrow 6^2P_{3/2}$, $F' = 5$. This can be explained by noting that different detunings also lead to the changing of the scattered force.[39,42] We eventually find the best parameters to obtain the maximum number of atoms in the MOT: the intensity of the cooling beams is 23.5 mW/cm^2, the intensity of the re-pumping beam is 7.1 mW/cm^2, the detuning of the cooling beam is −13.0 MHz, and the axial magnetic gradient is 9.7 Gauss/cm.

4. Conclusion and perspectives

In conclusion, we have experimentally demonstrated that a nanofiber can be used to optimize the number of atoms in a MOT. The nanofiber is a very good tool to collect and guide the photons emitted even with a very small number of trapped atoms. Optimal parameters based on our experimental system for the maximum number of cold cesium atoms are obtained. The performance of this method in optimizing the MOT is reliable and the result is consistent with previous work by conventional methods.[43,44] In contrast with convention methods, we can reliably monitor the cold atoms in a MOT in real time by using nanofibers, because the fluorescence collection efficiency is high.[7] It is possible to use the nanofibers to calibrate MOT number. The density distribution of the atomic cloud in MOT can be estimated using a nanofiber.[28] Because the diameter of the nanofiber is very small (just a few hundreds of nanometers), one-dimensional density distribution of the atomic cloud in MOT can be estimated with high spatial resolution. This method provides a way toward quantum precision measurement based on the manipulation of atom-photon interaction. In addition, due to the efficient coupling, nanofibers can be used to monitor and manipulate cold atoms as a powerful tool in quantum optics, atom physics, and hybrid quantum systems.[23,45–47] Nanofibers can also be integrated into optical fiber communication systems. When taken together with cold atoms, such nanofiber-based atom–photon systems have great potential in quantum memory[48] and quantum communications.[49]

Acknowledgments

The authors would like to thank Chang-ling Zou and Dandan Sun for helpful discussions.

References

[1] Kien F L, Liang J Q, Hakuta K and Balykin V I 2004 *Opt. Commun.* **242** 445
[2] Nayak K P, Sadgrove M, Yalla R, Kien F L and Hakuta K 2018 *J. Opt.* **20** 073001
[3] Tong L, Zi F, Guo X and Lou J 2012 *Opt. Commun.* **285** 4641
[4] Wu X and Tong L 2013 *Nanophotonics* **2** 407
[5] Solano P, Grover J A, Hoffman J E, Ravets S and Fatemi F K 2017 *Adv. At. Mol. Opt. Phys.* **66** 439
[6] Tong L, Gattass R R, Ashcom J B, He S, Lou J, Shen M, Maxwell I and Mazur E 2003 *Nature* **426** 816
[7] Kien F L, Dutta Gupta S, Balykin V I and Hakuta K 2005 *Phys. Rev. A* **72** 032509
[8] Phillips W D and Metcalf H 1982 *Phys. Rev. Lett.* **48** 596
[9] Chu S, Hollberg L, Bjorkholm J E, Cable A and Ashkin A 1985 *Phys. Rev. Lett.* **55** 48
[10] Dalibard J and Cohen-Tannoudji C 1989 *J. Opt. Soc. Am. B* **6** 2023
[11] Saffman M, Walker T and Molmer K 2010 *Rev. Mod. Phys.* **82** 2313
[12] Wang L, Zhang H and Zhang L J 2018 *J. Quantum Opt.* **24** 178 (in Chinese)
[13] Anderson M H, Ensher J R, Matthews M R, Wieman C E and Cornell E A 1995 *Science* **269** 198
[14] Yang G Y, Chen L C, Mi C D, Wang P J and Zhang J 2018 *J. Quantum Opt.* **24** 156 (in Chinese)
[15] Reiserer A and Rempe G 2015 *Rev. Mod. Phys.* **87** 1379
[16] Wang Y, Zheng R F, Zhang H and Zhou L 2018 *J. Quantum Opt.* **24** 436 (in Chinese)
[17] Monroe C and Lukin M 2008 *Phys. World* **21** 32
[18] Wang Y H, Yang H J, Zhang T C and Wang J M 2006 *Acta Phys. Sin.* **55** 3403 (in Chinese)
[19] Gibble K E, Kasapi S and Chu S 1992 *Opt. Lett.* **17** 526
[20] Weiner J, Bagnato V S, Zilio S and Julienne P S 1999 *Rev. Mod. Phys.* **71** 1
[21] Vengalattore M, Conroy R S and Prentiss M G 2004 *Phys. Rev. Lett.* **92** 183001
[22] Stites R, McClimans M and Bali S 2005 *Opt. Commun.* **248** 173
[23] Lin Y W, Chou H C, Dwivedi P P, Chen Y C and Yu I A 2008 *Opt. Express* **16** 3753
[24] Kien F L, Balykin V I and Hakuta K 2006 *Phys. Rev. A* **73** 013819
[25] Kien F L, Balykin V I and Hakuta K 2006 *Phys. Rev. A* **74** 033412
[26] Nayak K P, Melentiev P N, Morinaga M, Kien F L, Balykin V I and Hakuta K 2007 *Opt. Express* **15** 5431
[27] Nayak K P and Hakuta K 2008 *New J. Phys.* **10** 053003
[28] Sague G, Vetsch E, Alt W, Meschede D and Rauschenbeutel A 2007 *Phys. Rev. Lett.* **99** 163602
[29] Kien F L and Hakuta K 2009 *Phys. Rev. A* **80** 053826
[30] Nayak K P, Kien F L, Kawai Y, Hakuta K, Nakajima K, Miyazaki H and Sugimoto Y 2011 *Opt. Express* **19** 14040
[31] Wuttke C, Becker M, Bruckner S, Rothhardt M and Rauschenbeutel A 2012 *Opt. Lett.* **37** 1949
[32] Nayak K P and Hakuta K 2013 *Opt. Express* **21** 2480
[33] Yalla R, Sadgrove M, Nayak K P and Hakuta K 2014 *Phys. Rev. Lett.* **113** 143601
[34] Schneeweiss P, Zeiger S, Hoinkes T, Rauschenbeutel A and Volz J 2017 *Opt. Lett.* **42** 85
[35] Cheng F, Zhang P F, Wang X and Zhang T C 2017 *J. Quantum Opt.* **23** 74 (in Chinese)
[36] Zhang P F, Cheng F, Wang X, Song L J, Zou C L, Li G and Zhang T C 2018 *Opt. Express* **26** 31500
[37] Abraham E R I and Cornell E A 1998 *Appl. Opt.* **37** 1762
[38] Zhang P F, Li G, Zhang Y C, Guo Y Q, Wang J M and Zhang T C 2009 *Phys. Rev. A* **80** 053420
[39] Lindquist K, Stephens M and Wieman C 1992 *Phys. Rev. A* **46** 4082
[40] Hoth G W, Donley E A and Kitching J 2013 *Opt. Lett.* **38** 661
[41] Petrich W, Anderson M H, Ensher J R and Cornell E A 1994 *J. Opt. Soc. Am. B* **11** 1332
[42] Grego S, Colla M, Fioretti A, Müller J, Verkerk P and Arimondo E 1996 *Opt. Commun.* **132** 519
[43] Weiner J, Bagnato V S, Zilio S and Julienne P S 1999 *Rev. Mod. Phys.* **71** 1
[44] Haw M, Evetts N, Gunton W, Dongen J V, Booth J L and Madison K W 2012 *J. Opt. Soc. Am. B* **29** 475
[45] Vetsch E, Reitz D, Sague G, Schmidt R, Dawkins S T and Rauschenbeutel A 2010 *Phys. Rev. Lett.* **104** 203603
[46] Goban A, Choi K S, Alton D J, Ding D, Lacroute C, Pototschnig M, Thiele T, Stern N P and Kimble H J 2012 *Phys. Rev. Lett.* **109** 033603
[47] Kato S and Aoki T 2015 *Phys. Rev. Lett.* **115** 093603
[48] Gouraud B, Maxein D, Nicolas A, Morin O and Laurat J 2015 *Phys. Rev. Lett.* **114** 180503
[49] Kimble H J 2008 *Nature* **453** 1023